

Repeated injections of ^{131}I -rituximab show patient-specific stable biodistribution and tissue kinetics

Cristian Antonescu¹, Angelika Bischof Delaloye¹, Marek Kosinski^{1, 2}, Pascal Monnin², Andreas O. Schaffland¹, Nicolas Ketterer³, Carine Grannavel¹, Tibor Kovacsovic⁴, Francis R. Verdun², Franz Buchegger^{1, 5}

¹ Service of Nuclear Medicine, University Hospital of Lausanne, Rue du Bugnon 46, 1011, Lausanne, Switzerland

² Institute of Applied Radiophysics, University of Lausanne, Lausanne, Switzerland

³ Multidisciplinary Oncology Center, University Hospital of Lausanne, Lausanne, Switzerland

⁴ Center for Hematological Malignancies, Oregon Health and Science University, Portland, OR, USA

⁵ Service of Nuclear Medicine, University Hospital of Geneva, Geneva, Switzerland

Received: 6 January 2005 / Accepted: 17 February 2005 / Published online: 12 April 2005

© Springer-Verlag 2005

Abstract. *Purpose:* It is generally assumed that the biodistribution and pharmacokinetics of radiolabelled antibodies remain similar between dosimetric and therapeutic injections in radioimmunotherapy. However, circulation half-lives of unlabelled rituximab have been reported to increase progressively after the weekly injections of standard therapy doses. The aim of this study was to evaluate the evolution of the pharmacokinetics of repeated ^{131}I -rituximab injections during treatment with unlabelled rituximab in patients with non-Hodgkin's lymphoma (NHL).

Methods: Patients received standard weekly therapy with rituximab (375 mg/m^2) for 4 weeks and a fifth injection at 7 or 8 weeks. Each patient had three additional injections of $185\text{ MBq }^{131}\text{I}$ -rituximab in either treatment weeks 1, 3 and 7 (two patients) or weeks 2, 4 and 8 (two patients). The 12 radiolabelled antibody injections were followed by three whole-body (WB) scintigraphic studies during 1 week and blood sampling on the same occasions. Additional WB scans were performed after 2 and 4 weeks post ^{131}I -rituximab injection prior to the second and third injections, respectively.

Results: A single exponential radioactivity decrease for WB, liver, spleen, kidneys and heart was observed. Biodistribution and half-lives were patient specific, and without significant change after the second or third injection compared with the first one. Blood $T_{1/2\beta}$, calculated from the sequential blood samples and fitted to a bi-exponential curve, was similar to the $T_{1/2}$ of heart and liver but shorter than that of WB and kidneys. Effective radiation dose calculated from attenuation-corrected WB scans and blood using MIRDose3.1 was $0.53 \pm 0.05\text{ mSv/MBq}$ (range 0.48–

0.59 mSv/MBq). Radiation dose was highest for spleen and kidneys, followed by heart and liver.

Conclusion: These results show that the biodistribution and tissue kinetics of ^{131}I -rituximab, while specific to each patient, remained constant during unlabelled antibody therapy. RIT radiation doses can therefore be reliably extrapolated from a preceding dosimetry study.

Keywords: ^{131}I -rituximab – Repeated injections – Biodistribution – Pharmacokinetics

Eur J Nucl Med Mol Imaging (2005) 32:943–951

DOI 10.1007/s00259-005-1798-8

Introduction

The unlabelled chimeric monoclonal antibody (MAb) rituximab (Mabthera) and two radiolabelled mouse MABs, ibritumomab tiuxetan (Zevalin) and tositumomab (Bexxar), all directed against the CD20 antigen, have been approved for the treatment of non-Hodgkin's lymphoma (NHL). Radioimmunotherapy (RIT) with Zevalin [1, 2] uses ^{90}Y -labelled mouse MAb 2B8, combined with two administrations of 250 mg/m^2 unlabelled chimeric MAb C2B8 (rituximab). Bexxar treatment [3–5] is based on injection of ^{131}I -labelled mouse MAb anti-B1 combined with two administrations of 450 mg per patient of the same unlabelled MAb.

The number of reports on RIT of lymphoma is rapidly increasing [6–8]. Besides the approved radiopharmaceuticals, ^{131}I -rituximab has been used in low- and high-dose RIT [9–11]. First in vitro and in vivo alpha-radiation therapy experiments using DTPA-rituximab, labelled with ^{213}Bi and ^{149}Tb , have also been reported [12, 13].

Both approved RITs are based on the injection of a single therapeutic dose of radiolabelled mouse MAb that may be preceded by the injection of a dosimetric dose of MAb,

Franz Buchegger (✉)

Service of Nuclear Medicine, University Hospital of Lausanne,
Rue du Bugnon 46, 1011, Lausanne, Switzerland

e-mail: Franz.Buchegger@chuv.ch

Tel.: +41-21-3144373, Fax: +41-21-3144349

Table 1. Patient characteristics

Patient	Sex	Age (years)	Lymphoma type	Pre-treatment history
1 ^a	Female	58	Diffuse large B-cell lymphoma	Three chemotherapies including intensification, rituximab, radiotherapy (2 years' evolution) ^b
2	Male	45	Follicular lymphoma	Radiotherapy, four chemotherapies including intensification (10 years' evolution)
3	Male	67	Diffuse large B-cell lymphoma	Radiotherapy, two chemotherapies (2 years' evolution)
4	Male	73	Anaplastic diffuse large B-cell lymphoma	Two chemotherapies (10 years' evolution)

^aPatients 1 and 4 had ¹³¹I-rituximab injection at Mabthera treatment weeks 1, 3 and 7 and patients 2 and 3 at weeks 2, 4 and 8

^bPatient 1 also suffered from an invasive breast cancer, treated with radiotherapy before inclusion in this study

labelled with ¹¹¹In in the case of Zevalin and with ¹³¹I in that of Bexxar. In heavily pretreated patients, the appearance of human anti-mouse IgG antibodies (HAMA) has been observed in 17% after treatment with Bexxar antibody [4] and in a lower percentage (2%) after therapy with Zevalin [2]. However, upfront treatments of chemotherapy-naïve patients or repeated treatment cycles with mouse monoclonal antibodies might be more immunogenic. In contrast, after standard rituximab treatment with four weekly injections in patients having had previous chemotherapies, human anti-chimeric IgG antibodies (HACA) have been observed in less than 1%.

Dosimetry evaluation of RIT is frequently performed in a dosimetry study preceding the RIT, since it cannot be performed directly under therapy conditions because the gamma-radiation is either too high in the case of ¹³¹I-labelling or absent in the case of ⁹⁰Y-labelling. However, it has been reported that the blood half-life of unlabelled rituximab progressively increases after the successive injections during therapy [14, 15]. The reason for the prolongation of the blood half-life of unlabelled rituximab has not been entirely elucidated, though saturation of the easily accessible antigenic sites may be partially responsible. Dosimetric data obtained during a first administration of rituximab may be unable to predict the radiation exposure of the patient in a subsequent RIT performed 1–2 weeks later if half-life prolongation also occurs for the radiolabelled antibody. This is even more important when intending to administer multiple RIT courses in order to increase the total administered activity while limiting toxicity.

With the intention of delivering repeated courses of RIT with radiolabelled rituximab, in this study we investigated the biodistribution and kinetics of ¹³¹I-rituximab after repeated injections during standard rituximab therapy in patients with lymphoma. Repeated injections of diagnostic doses of ¹³¹I-rituximab were performed in weeks 1, 3 and 7 or 2, 4 and 8, respectively. All injections were followed by standardised, sequential anterior and posterior whole-body (WB) scintigraphic studies and blood sampling.

Materials and methods

Patients

Evolution of the biokinetics of repeated radiolabelled antibody injections was studied in four patients (one female and three males), aged 60.8±12.2 years, with relapsed NHL after having obtained written informed consent. Patient characteristics and their lymphoma history are shown in Table 1. Inclusion criteria included adequate renal and hepatic functions (aspartate aminotransferase, bilirubin and creatinine were not to exceed twice the upper normal limit, i.e. <100 U/l, <42 µmol/l and <212 µmol/l, respectively) and a negative HAMA test. The study protocol had been approved by the local Ethics Committee and the Swiss authorities (Swissmedic and the Federal Office of Public Health, Section of Radioprotection).

Antibody radiolabelling

The 12 radiolabellings were performed adopting the rules of good clinical practice (GCP) as described [16]. Briefly: 0.2 ml clinical grade rituximab (2 mg) solution, provided by Roche Pharma (Reinach, Switzerland), and 100 µl freshly prepared chloramine T solution (50 µg per 0.1 ml 0.15 M sterile phosphate buffer pH 7) were added to 370 MBq Na¹³¹I solution (no-carrier-added Na¹³¹I in phosphate buffer, MDS Nordion S.A., Fleurus, Belgium), previously diluted to 200 µl with 0.15 M phosphate buffer pH 7.0. After 5 min at room temperature, labelling efficacy was controlled by thin-layer chromatography (ITLC, methanol/0.9% saline=85/15) and the labelling solution pumped at 0.5 ml/min flow through a Dowex resin filter column [1.8 g anion exchange resin (Dowex 1×8–100) in a 2-ml reversible tube (Supelco, Buchs, Switzerland) in sterile 0.9% NaCl solution] into a new vial. The purified radiolabelled antibody solution was sterile filtered (MILLEX-GV 0.22-µm millipore filters, Millipore Corp., Bedford, MA, USA) into a sterile penicillin vial for clinical use. Sterility was demonstrated for three sequential assays before radiolabellings were performed for injection of patients. Foreseeing use of this radiolabelling procedure for therapy, a semi-automatic set-up was chosen for antibody labelling and purification [16].

Chemicals and solvents were from Merck (Dietikon/ZH, Switzerland) and Fluka (Buchs, Switzerland). Analytical size-exclusion high-performance liquid chromatography (HPLC) was performed on a guard-protected TSK-Gel column: TSK 3000 SW 300 mm×7 mm (Toyo Soda Manufacturing Co., Yamaguchi, Japan). Thin-layer chromatograms (Pall Corp., Ann Arbor, USA) were scanned on a Berthold LB 284 linear analyser.

Binding assay

Immunoreactivity of the 12 freshly radiolabelled antibody preparations was measured without delay in duplicates on Daudi lymphoblastoma B cells in the exponential growth phase using five sequential dilutions between one and 10×10^6 cells. Daudi cells (American Type Culture Collection ATCC) are well known for surface expression of the CD20 antigen. Cells were cultured in RPMI 1640 medium+Glutamax I, containing 10% foetal calf serum, penicillin and streptomycin. First results of a Scatchard determination indicated the presence of 9.2×10^4 antibody binding sites per cell and an affinity K_a of ^{131}I -rituximab of 3.0×10^8 l/M, well compatible with the reported affinity of ^{125}I -rituximab [17], suggesting that the immunoreactivity had been preserved.

For binding determination, 6 ng (1 kBq) of ^{131}I -rituximab was incubated at 37°C for 2 h with Daudi cells in a volume of 200 µl PBS (0.15 M NaCl and 0.01 M phosphate buffer pH 7) containing 2% foetal calf serum. After two washings, cell-bound radioactivity was counted in comparison to a 100% standard sample and expressed in % of total input activity. Non-specific binding (generally <3%) was assessed by competition with 100 µg unlabelled antibody and subtracted for determination of specific binding. Specific binding results were expressed as maximal observed binding on 10^7 fresh Daudi cells and using extrapolation to infinite antigen excess according to Lindmo et al. [18].

Patient injection and data collection

Patients had standard weekly therapy with rituximab for 4 weeks and a fifth injection at 7 or 8 weeks. The standard therapy doses of unlabelled rituximab (375 mg/m^2) were infused over 2–3 h. Each of the four patients had three additional injections of fresh radiolabelled ^{131}I -rituximab in either treatment weeks 1, 3 and 7 (two patients) or weeks 2, 4 and 8 (two patients). ^{131}I -rituximab (185 MBq) injections were performed over 30 min immediately after injection of unlabelled antibody, except for the first radiolabelled antibody injection in patients 1 and 4, where the ^{131}I -rituximab was scheduled 24 h after the first administration of unlabelled rituximab. This procedure takes into account the higher incidence of adverse reactions observed during the first rituximab infusion. Standard precautions were used during injection, including frequent control of vital parameters. Patients were scanned with a large field of view dual-head BIA camera (Trionix, Twinsburg, Ohio) equipped with high-energy parallel collimators and using a matrix of $1,024 \times 256$. Camera uniformity, background and the energy peaks were checked daily.

Scanning procedure was performed as described by Wahl et al. [19]: Prior to all patient scans, one scan of background activity and another scan of a stored ^{131}I standard sample (a standard of ~8 MBq was prepared at day 0, in 10 ml solution) were recorded using a scan speed of 10 cm/min, a scan length of 200 cm and an energy peak of 364 keV with a window of 28%, using predefined positions of camera heads, table and standard sample. The patient was then scanned under identical conditions, on day 0 immediately after antibody perfusion (without bladder voiding, 100% reference scan), on day 2, 3 or 4 and on day 6 or 7 (after bladder voiding). In patients 1, 2 and 3, additional scintigraphic studies were performed just before the perfusion of the second and third radiolabelled antibody injections.

The standard sample scans and the patient WB scans were corrected for background activity, measured on the same day. The background corrected activities of day 2, 3 or 4 and day 6 or 7 were expressed in % of activity measured on day 0. Regions of interest (ROIs) of organs were determined, and geometric means of anterior

and posterior scintigraphic studies used for half-life and dosimetry determinations.

Blood samples were obtained before each radiolabelled antibody injection and at 15 min (100% reference) and 2 h post injection as well as at the time of the second and third WB scans. A standard of injected activity allowed back-calculation of total blood volume distribution of the injected radiolabelled antibody. Blood and plasma radioactivity was determined in a gamma counter (Wizard, PerkinElmer, Wallac OY, Turku, Finland) together with the standard radioactivity sample.

Tissue and blood radioactivity kinetics

WB and tissue activities of the first 6–7 days post injection were fitted to a single exponential curve, since no reproducible deviation from that curve was observed.

Blood half-lives α and β were determined by fitting measured activity data to a bi-exponential curve according to the formula:

$$\text{Activity}(t) = A_1 \cdot e^{-\lambda_1 t} + A_2 \cdot e^{-\lambda_2 t}$$

where A_1 is the fractional activity exhibiting half-life $\alpha = \ln 2 / \lambda_1$ and A_2 is the fractional activity exhibiting half-life $\beta = \ln 2 / \lambda_2$.

Dosimetry

Dosimetry was performed using Mirdose3.1 [20] based on the data of the 12 injections from the four patients. Residence times for WB, liver, kidneys, spleen and heart were calculated from the ROIs based on geometric means of anterior and posterior scintigraphic studies and using single exponential decrease of activity. Activity was corrected for attenuation with an attenuation factor of 0.12 cm^{-1} , using, where available, organ and body sizes measured by CT and otherwise standard organ sizes and a body thickness of 21 cm. Bone marrow (BM) residence time was calculated from blood activity according to the formula proposed [21]:

$$t_{rm} = t_{\text{blood}}(m_{rm}/m_{\text{blood}})(0.19/(1 - \text{hematocrit}))$$

where t is the residence time of blood and marrow, respectively, rm is red marrow and m is the mass of blood or red marrow, respectively. Red marrow mass was set at 1,120 and 1,050 g, respectively, for the standard human phantoms of 70 and 57 kg [20]. Residence times of the four organs, red marrow and rest of the body were then used for calculation of radiation doses with Mirdose3.1 [20], using the phantom closest to the patient effective weight. Mirdose results were then extrapolated to effective patient weight using mathematical inverse proportions of weight and dose.

HAMA assay

In the absence of a commercially available HACA assay, a HAMA assay (HAMA Elisa, Medac, Hamburg, Germany) was performed for all four patients and was always negative. The HAMA assay was repeated at 3 and 6 months after the first injection of the radiolabelled Mab. Though not entirely covering the potential occurrence of HACA, the HAMA assay may detect anti-HACA antibodies in many patients since they can be directed against the mouse IgG framework of the variable domains.

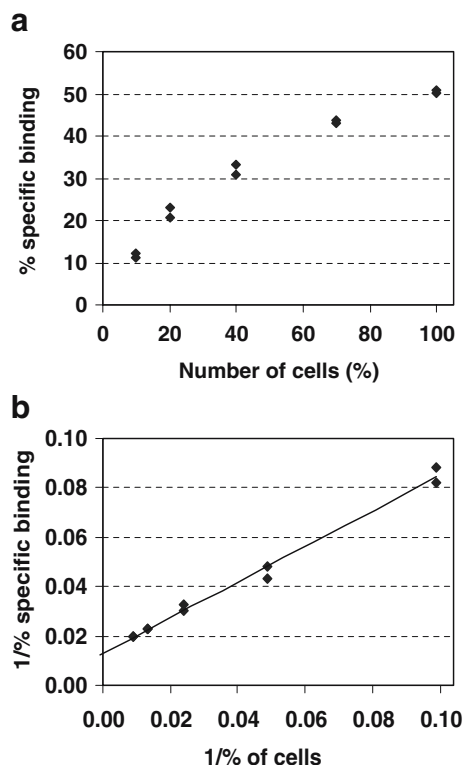


Fig. 1. Specific binding results (duplicates, non-specific binding has been subtracted) are shown in **a** as obtained by incubation with five dilutions of Daudi cells. The same results are shown in **b** in double inverse plot according to Lindmo et al. [18], allowing extrapolation of the maximal binding that would be obtained at infinite antigen excess. While in **a** the maximal observed binding was 50.6%, in **b** the intercept with the ordinate of the linear regression straight line, defined as $y=0.719x+0.0124$ ($r^2=0.99$), gives the reciprocal result of the maximal theoretical binding of ^{131}I -rituximab, in this case 80.6%

Statistical analysis

Statistical comparisons were first performed using Student's *t* test. The multigroup comparisons were then performed with the ANOVA analysis of variance to determine the potential prevalence of significant subgroup differences. In the case of significant differences between subgroups, these were sorted out by the subsequent Tukey test.

Results

^{131}I -labelling of rituximab and immunoreactivity

The 12 radiolabelled antibody fractions were prepared using ^{131}I within 2 days of calibration. The radiochemical yield of ^{131}I -rituximab was $91.7\pm 4.2\%$. The radiochemical purity after anion exchange chromatography of ^{131}I -rituximab, assessed by TLC ($n=12$), was $99.1\pm 0.5\%$. These results were confirmed using size-exclusion HPLC ($n=5$), which showed a radiochemical purity of ^{131}I -rituximab of $98.9\pm 0.9\%$ and $0.6\pm 0.5\%$ of aggregates, not significantly different from the results for unlabelled precursor antibody. Storage at 4°C for up to 8 h post labelling revealed the

absence of any further aggregation or degradation products; antibody injections were performed within 2 h from preparation. Upon longer storage for 24 h at 4°C , formation of maximally 3% aggregates was observed (results not shown).

Immunoreactivity of the preparations ($n=12$) was determined immediately after labelling by incubation with fresh cultured Daudi cells in exponential growth phase. Mean specific binding as measured on 10^7 cells was $48.3\pm 9.0\%$. Using extrapolation to infinite antigen excess according to Lindmo et al. [18], a mean immunoreactivity of $72.2\pm 15.2\%$ was calculated (Fig. 1). First results of an affinity determination according to Scatchard linearisation [22] indicated a K_a of 3.0×10^8 l/M, similar to the reported affinity of 1.9×10^8 l/M for ^{125}I -labelled rituximab [17].

Camera controls

Camera quality controls included a test of uniformity and two scans performed under identical conditions as defined for patient WB scans (scan length of 2 meter, identical position of camera heads and bed), once with a standard activity sample of 8 MBq ^{131}I (prepared at day 0 and re-used for subsequent scans) and once for background determination. Camera measurement in the calibration setting and after background subtraction at day 0 gave $6.04\pm 0.14\times 10^3$ counts/MBq ($n=12$). Setting the initial measurements at day 0 as 100%, subsequent calibration measurements between days 2 and 7 were at $99.3\pm 1.6\%$ (range 96.4–103.4%, $n=24$) of the predicted value calculated from the ^{131}I decay (Fig. 2).

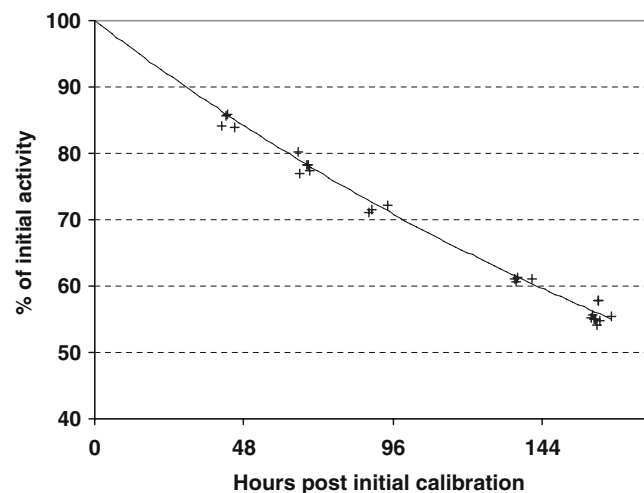
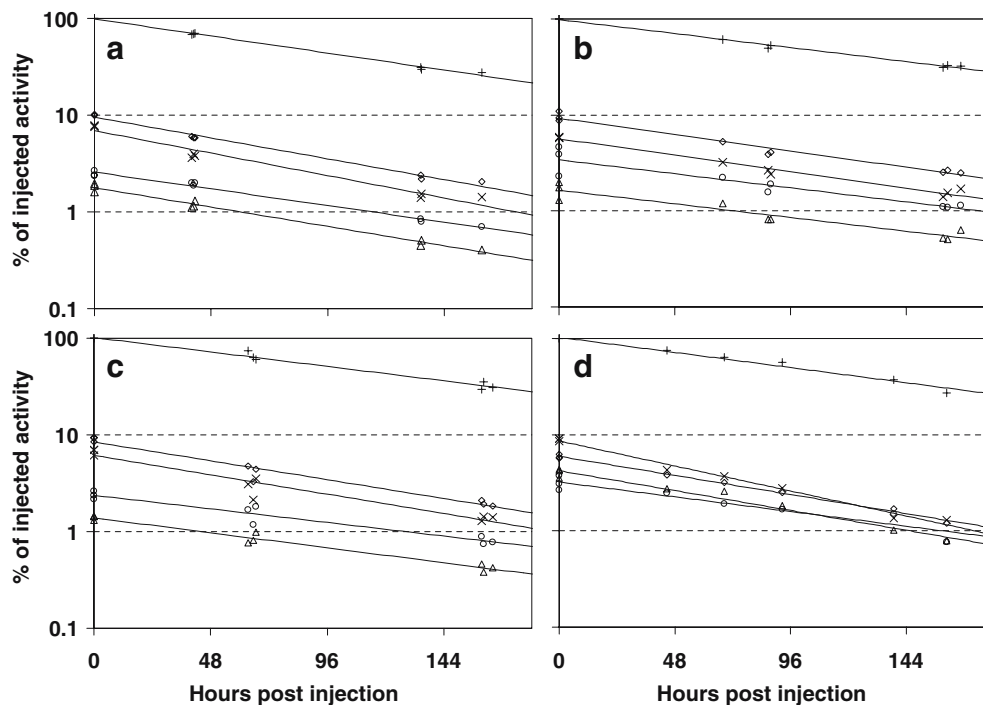


Fig. 2. Gamma camera quality control. On the days of patient scanning, two control scans were performed, one with a ^{131}I standard sample prepared at day 0, and one of background, using identical parameters as defined for patient WB scans. Taking the background-subtracted scanning results of the ^{131}I standard sample at day 0 as 100%, subsequent results were expressed in % of initial activity and plotted against hours post initial calibration. The thin line shows the theoretical exponential decrease in ^{131}I activity. Note that the observed results were all in between 96.4% and 103.4% of the expected result

Fig. 3. WB (+), liver (\diamond), heart (x), kidney (\circ) and spleen (Δ) results are shown as obtained from the four patients and the three injections in each based on anterior and posterior geometric means corrected for attenuation. **a, b, c** and **d** represent data from patients 1, 2, 3 and 4, respectively. Only mean single exponential decreases per patient are shown, each fitted to the nine scan results available per patient. The corresponding half-lives calculated for the three individual injections per patient are given in Table 3



WB and tissue kinetics

The 12 radiolabelled antibody injections were well tolerated. After each injection, WB and tissue distributions and biokinetics were determined using three WB scintigraphic studies performed over 1 week. WB activity decrease was determined using geometric means of anterior and posterior WB scans including background and attenuation correction. This determination gave a mean $T_{1/2}$ of 92.0 ± 7.7 h (range 81.5–99.0 h, Fig. 3, Table 2). When the half-lives after each injection were analysed, a small intra-patient coefficient of variation (CV) was observed (mean CV=5.9%).

Using background-corrected anterior WB scans as reported previously [19], WB radioactivity measurements also showed a single exponential decrease (results not shown). The average $T_{1/2}$ was 92.9 ± 9.2 h (range 80.7–103.0 h for individual patients), very similar to the results derived from the anterior and posterior scans. Intra-patient variation in

WB $T_{1/2}$ after the three injections was small in this analysis, too, with a CV ranging from 2.9% to 4.7%.

Tissue radioactivity of liver, spleen, kidneys and heart followed a single exponential decrease (Fig. 3). In individual patients, no major change and in particular no systematic prolongation of the effective tissue $T_{1/2}$ appeared to occur after the repeated applications of ^{131}I -rituximab.

Blood radioactivity showed a bi-exponential decrease that was calculated on the combined results of the three injections per patient (Fig. 4), since in individual patients activity of the samples after the three injections showed only small deviations from the mean calculated value. Effective $T_{1/2\alpha}$ was short (mean= 6.0 ± 2.4 h, range 4.1–9.4 h), similar to the $T_{1/2\alpha}$ observed for other radiolabelled antibodies. The fraction of activity A_1 with $T_{1/2\alpha}$ was 39.2% (range 33.6–44.1%) as compared with the total activity. While the effective $T_{1/2\beta}$ of blood was rather long (range 64.6–82.2 h, Table 2), it was shorter than the mean WB

Table 2. Average effective tissue half-lives (h) are shown as calculated from attenuation-corrected WB scans from the first 6–7 days post injection in comparison with the mean blood effective $T_{1/2\beta}$

Patient	WB	Heart	Blood	Liver	Spleen	Kidneys
1	99.0	84.5 ^a	82.2 ^a	84.5 ^a	101.9 ^b	99.0
2	81.5	62.4	66.9	66.6	72.2	83.5
3	96.3	72.2	73.3	73.7	93.7	101.9
4	91.2	57.3	64.6	73.0	70.7	92.4
Mean \pm 1 SD	92.0 \pm 7.7	69.1 \pm 12.0	71.8 \pm 7.9	74.5 \pm 7.4	84.6 \pm 15.6	94.2 \pm 8.2

^aThe half-lives for heart, liver and blood are strikingly similar in the four patients and different from those for WB and kidneys. ANOVA followed by the Tukey test demonstrated a significant difference for the heart compared with kidneys (confidence value >95%), while the other mentioned differences showed a tendency towards significance

^bSpleen activity is variable compared with the other tissues, possibly indicating variable binding of the antibody to CD20-expressing cells

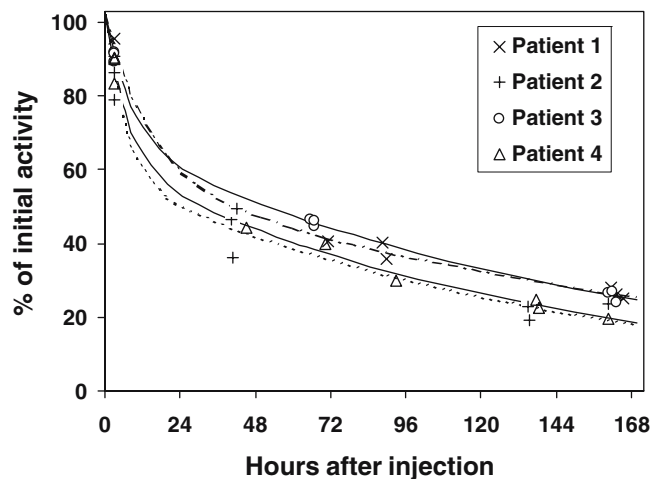


Fig. 4. Relative blood time-activity curves are shown, normalised to initial activity. Mean effective $T_{1/2\alpha}$ and β for each patient were determined by fitting the 12 measurements from the three injections per patient to bi-exponential curves

half-lives. Similar observations to those in blood were made in plasma (results not shown).

Average effective tissue $T_{1/2}$ and blood $T_{1/2\beta}$ of individual patients (Table 2) suggested the presence of two groups of results, one including WB and kidneys with a longer half-life and the other, blood, heart and liver with a shorter half-life. The ANOVA test showed a significant difference (confidence interval >95%) for the comparison of heart with kidneys while the other comparisons of the two groups showed a tendency towards a difference (confidence interval <95%). Spleen half-lives appeared variable compared with the half-lives of the other tissues, blood and WB. This variability might have been due to differential expression of CD20 on target cells.

Data shown in Table 2 were resolved for the half-lives after the three individual injections per patient (Table 3) and comparatively analysed for statistical differences between injections and between patients, respectively. Since the $T_{1/2\alpha}$ would only marginally influence blood activity beyond 2 days after injection, a single exponential decrease was assumed to occur between the blood samples of day 2, 3 or 4 and day 6 or 7, and an approximate $T_{1/2\beta}$ could be determined for the individual injections. The results showed only minor variations (mean CV=7.8%) in individual patients (Table 3).

The analysis of individual injections per patient showed that the overall mean $T_{1/2}$ values were very similar after the three injections (Table 3). ANOVA showed the absence of any significant difference between the three injections, with the 95% confidence intervals ranging from 76 to 89, 74 to 91 and 75 to 86 h, respectively, for injections 1, 2 and 3, far from any tendency towards significance ($p>0.8$).

When analysing the same data on a per patient basis, the half-lives after the second and/or third injection compared with the first one showed some marginal decreases in patients 3 and 4 and slight increases in patients 1 and 2. However, these variations were rather random and not significant, with $p>0.4$ for the four analyses. Finally, an analysis of the

half-life data from blood and heart did not show any significant difference either ($p>0.6$). Overall, also on a per patient basis or for blood and heart, no significant increase or decrease in half-lives was observed in regard to the data of Table 3.

In contrast, when the same results were sorted in a patient to patient comparison ($n=18$ for each patient), the mean half-lives of patients 1 and 3 ($T_{1/2}=93.2\pm 18.7$ h and 85.7 ± 14.6 h, respectively) appeared longer compared with those of patients 2 and 4 ($T_{1/2}=71.9\pm 9.0$ h and 76.7 ± 15.7 h, respectively). ANOVA followed by the Tukey test confirmed that the half-lives of patient 1 were significantly longer than those of patients 2 and 4 (confidence interval >99%). For patient 3, the half-lives were significantly longer than those of patient 2 (confidence interval >95%), while the comparison of patients 3 and 4 showed only a tendency towards a difference (confidence interval <95%).

Additional scans had been performed in three patients at 2 and 4 weeks after the first and second injections, respectively. The results suggested that a minor fraction of radioactivity might have a longer half-life than the one extrapolated from the first 7 days since in two of the three patients background-corrected WB activity at 2 and 4 weeks

Table 3. Effective half-lives for individual organs and tissues as calculated for individual injections. Blood effective $T_{1/2\beta}$ was estimated from samples obtained 2–7 days post injection, as explained

Organ/tissue	Patient	Injection I	Injection II	Injection III
Liver	1	78.8	88.9	87.7
	2	61.9	71.7	66.0
	3	77.0	75.3	70.7
	4	79.6	68.0	76.2
Heart	1	95.0	77.0	83.5
	2	59.8	68.0	56.3
	3	80.6	66.6	70.0
	4	51.3	60.8	60.3
Spleen	1	100.5	121.6	90.0
	2	72.9	70.0	72.2
	3	92.4	100.5	87.7
	4	79.7	65.4	71.5
Kidneys	1	84.3	150.7	86.6
	2	81.5	81.5	87.7
	3	115.5	101.9	93.7
	4	100.5	77.9	108.3
Blood	1	80.3	66.9	88.9
	2	62.8	71.0	67.3
	3	69.5	73.4	75.1
	4	73.0	64.9	64.5
WB	1	101.9	95.0	100.5
	2	77.9	85.6	80.6
	3	106.6	88.9	96.3
	4	99.0	84.5	95.0
Mean \pm 1 SD		82.6 \pm 16.1*	82.3 \pm 20.6*	80.7 \pm 13.5*

*The ANOVA did not indicate any significant difference between the three injections, with $p>0.8$ for these overall comparisons. When analysed on an individual patient basis, the fluctuations also remained random, with $p>0.4$ for the four patients

Table 4. Late WB activities (2 and 4 weeks after injection, respectively) of patients 1, 2 and 3 are shown in percent of injected activity (% ID), once as expected from the extrapolation of WB $T_{1/2}$ calculated from the results of the first 7 days post injection and once as observed values

Patient	1st injection, values at 2 weeks		2nd injection, values at 4 weeks	
	Extrapolated	Observed	Extrapolated	Observed
1	12.0	15.7	0.95	2.0
2	6.1	7.5	0.35	1.1
3	9.6	9.4	0.86	1.2

Note that in patients 1 and 2, the observed activities at 2 or 4 weeks post injection are slightly higher than the expected activities, while the results are concordant in patient 3

was slightly higher than the activity expected from the mean half-life calculated from the first week (Table 4).

Dosimetry and HAMA

Dosimetry was performed using Mirdose3.1 based on the WB and tissue results determined from all scintigraphic studies and using blood activity for determination of the bone marrow dose. The mean effective radiation dose for the four patients was calculated as 0.53 ± 0.05 mSv/MBq (range 0.48–0.59 mSv/MBq), the highest radiation dose being delivered to the spleen followed in decreasing order by kidneys, heart and liver (Table 5).

Absence of HAMA was verified in plasma samples obtained before the study (as an inclusion criterion) and at 3 and 6 months post treatment initiation. All patients were HAMA negative before entering the study and remained negative 3 and 6 months after the study.

Table 5. Mean tissue radiation doses (mGy/MBq) and the effective dose (mSv/MBq) are shown as calculated using Mirdose3.1 [20] from attenuation-corrected tissue distributions

	Patient				Mean \pm 1 SD
	1	2	3	4	
Liver	1.21	0.81	0.83	0.59	0.86 \pm 0.26
Kidneys	2.50	1.66	1.95	2.13	2.06 \pm 0.35
Spleen	2.26	1.65	1.69	3.41	2.25 \pm 0.82
Heart	1.46	1.27	1.42	1.88	1.51 \pm 0.26
Bone marrow	0.75	0.51	0.54	0.50	0.58 \pm 0.12
Total body	0.45	0.33	0.44	0.31	0.38 \pm 0.07
Effective dose (mSv/MBq)	0.50	0.53	0.59	0.48	0.53 \pm 0.05

Bone marrow radiation dose was calculated from blood activity measurements as proposed previously [21]

Discussion

The evolution of the biodistribution and tissue kinetics of radiolabelled antibodies in individual patients undergoing RIT of lymphoma in combination with unlabelled antibody treatment is an important parameter when considering repeated treatments. Furthermore, dosimetry estimates based on diagnostic imaging performed 1–2 weeks before RIT are only reliable if the tissue distribution and biokinetics of radiolabelled antibody do not change between the dosimetry study and RIT. It is generally assumed that these parameters remain constant in separate dosimetry and therapy phases. However, to our knowledge, only a few graphical presentations of blood activity measurements of ^{111}In -Zevalin compared with ^{90}Y -Zevalin have been presented [1] in support of this assumption.

In contrast to the aforementioned assumption, it has been reported that the blood half-life of rituximab increases progressively after successive injections in standard Mabthera treatment. The reported plasma half-life of rituximab increased from a mean of only 33 h after the first injection to 77 h after the fourth injection in one group of patients [15], and in another group it rose from an initial mean of 76 ± 31 h to 206 ± 95 h at the fourth injection [14]. A further report mentioned an average blood half-life of 226 h (range 13–371 h) in a selected group of patients [23].

An obvious possible explanation for the reported prolongation of the blood half-life after successive unlabelled antibody injections is that accessible antigen on normal B cells and tumour either is progressively saturated or disappears as cells die off. If this were the only explanation for increasing circulation times of unlabelled antibodies, a similar increase in blood and tissue half-lives would be expected to occur for simultaneously injected ^{131}I - or ^{90}Y -labelled antibodies. Such an increase in the biological half-life of radiolabelled rituximab would invalidate dosimetry measurements performed before RIT and would be a particular handicap when envisaging repeated RIT.

In the four patients studied here, in the framework of standard, unlabelled Mabthera treatment of lymphoma, the measured biodistribution and pharmacokinetics of repeated ^{131}I -labelled antibody injections remained constant in blood, plasma and heart, and in all measured tissues and total body, without any significant increase from the first to the second or third injection.

WB radioactivity measurements showed a single exponential decrease, with an average $T_{1/2}$ of 92.0 ± 7.7 h for the 12 injections. This is longer than the reported mean half-life of 59.3 h (range 24.6–88.6 h) observed for ^{131}I -tositumomab [4], which is a very effective treatment [24]. Very similar, overlapping WB half-lives of 3.2–7.5 days were reported recently for another chimeric ^{131}I -labelled antibody, G250 [25].

From the observed effective half-lives in blood, we calculated an average biological $T_{1/2\beta}$ of 113 h (range 97.4–142.8 h) for ^{131}I -rituximab. This blood kinetic is again similar to that reported for the ^{131}I -labelled chimeric Mab G250 [25]. As expected, this is markedly longer than the biological half-life of 48 h (range 18–77 h) reported for

¹¹¹In-Zevalin [1]. ¹¹¹In-Zevalin is the radiolabelled mouse MAb 2B8, parental to the chimeric rituximab C2B8. Blood and plasma biological $T_{1/2\beta}$ values in our study are also longer than the reported initial half-lives after the first infusion of unlabelled rituximab [14, 23], and yet we started our dosimetry phase in two patients with the first injection of unlabelled rituximab. The WB results presented here match well with reports of dosimetry studies of two other groups [10, 11], who reported average effective WB half-lives of 81 h (range 40–133 h) and 85.4 h (range 46–115 h), respectively, for ¹³¹I-rituximab labelled with specific activities between 27 and 74 MBq/mg antibody.

The observed stability of radiolabelled rituximab in terms of blood $T_{1/2\beta}$ and tissue half-lives in the course of the unlabelled rituximab treatment remains puzzling. Since radiolabelled rituximab represents only a small fraction of unlabelled rituximab in this biodistribution setting, as is also the case in RIT, one would expect the radiolabelled antibody in blood and tissues to behave similarly to the unlabelled antibody. This seems not to be the case, however. Different hypotheses may be suggested to explain the apparent discrepancy between our results with radiolabelled rituximab and those reported in the literature concerning unlabelled rituximab [14, 15]. It is to be mentioned that in standard rituximab treatment, an intentional rise in blood antibody titres is achieved by the weekly injections of unlabelled antibody, with the aim of prolonging therapeutic titres. Thus, at the time of the fourth injection, an important residual proportion of blood antibody from the third and second injections is already in the $T_{1/2\beta}$ phase, or possibly even in a third phase. The increase in the blood half-life of unlabelled rituximab could thus be partially explained by this cumulative effect.

In contrast to the observations with unlabelled rituximab [14, 15], in our study only minor amounts of radiolabelled antibody remained at the second and third injections from the respective previous injections. In fact, at the second ¹³¹I-rituximab injection the fraction remaining from the first injection (after a 2-week interval) was less than 15%, while at the third injection (after a 4-week interval) remaining activity was less than 2% (these fractions were determined in three of our four patients). Thus, in contrast to the measurements with unlabelled antibody, our biokinetic study of radiolabelled antibody essentially analysed the behaviour of freshly injected activity.

A second relevant observation concerns the fact that tissue and blood/plasma kinetics of ¹³¹I-rituximab were measured directly by radioactivity counting and WB scintigraphy, while the blood fractions of unlabelled antibody [14, 15] were determined immunologically. It is possible that the half-life of ¹³¹I-rituximab may have been shortened slightly by some dehalogenation, whereby unlabelled antibody would be generated. A further shortening of the half-life of radiolabelled antibodies may have occurred due to some degradation in the reticuloendothelial system (RES). We recently calculated that with a labelling of 185 MBq ¹³¹I per mg antibody, such as was used here, 0.87 iodine atoms were introduced per antibody molecule [16]. Despite this

low specific activity, a majority of radiolabelled antibodies were in fact calculated to contain two or more iodine atoms per antibody molecule [16]. This may have contributed to some clearing of radiolabelled antibodies in the RES. However, it is to be mentioned that none of the radiolabelled antibody fractions that were controlled by HPLC showed any damage that could be attributed to the radiolabelling procedure. Furthermore, the half-lives observed here are rather long, and dehalogenation or RES degradation, if either occurred, would have been of marginal relevance. Finally, the half-lives observed in this study are similar to those reported in two other studies using ¹³¹I-rituximab labelled at specific activities between 27 and 74 MBq per mg antibody [10, 11].

It could be argued that a biokinetic study using weekly injections of radiolabelled antibody might have given a different result owing to the cumulation of larger fractions of radiolabelled antibody remaining from preceding injections. While this is possibly true, such measurement was not the aim of this study. Instead, we considered that the difference of activity in the dosimetry and therapy phases with ¹³¹I-labelled rituximab is generally more than tenfold. Even after a short 7-day interval, the biokinetics of the therapeutic activity would be only marginally influenced by the low activity remaining from the dosimetry phase. Thus, separation of the repeated injections of ¹³¹I-rituximab in our study was justified by its usefulness for interpretation of RIT dosimetry and for the intended repetition of RIT, where injections are separated by more than 2–3 weeks. Furthermore, separation of injections by 2 or more weeks should allow more reliable detection of small increases in half-life than would be possible with an interval of 1 week between injections. This is particularly true for our study, since unlabelled antibody injections were continued weekly between the first and second injections of ¹³¹I-rituximab. Finally, the half-life of unlabelled rituximab [14, 23] was determined only after the first and fourth antibody injections.

Dosimetry was not a central aim of this study. However, it is well recognised that among dosimetry parameters, the blood-derived bone marrow dose underestimates the effective dose whenever CD20-expressing target cells, whether normal or tumoural, are present in red marrow and radiolabelled antibody is concentrated on these cells. While it has been repeatedly reported that normal B cells rapidly decrease in the blood after infusion of anti-CD20 antibody in therapeutic amounts, the consequence of this decrease for bone marrow accumulation of radiolabelled rituximab has not yet been investigated.

Tumour radiation dose was not evaluated in this study. Activity in regions containing tumour appeared to be similar after the repeated injections in individual patients; however, assessment of tumour radiation dose requires particular evaluations, notably volume determination in the case of small tumours. It remains a matter of debate whether tumour dose derived from sequential scintigraphic imaging and efficacy are correlated in lymphoma [26]. Normal tissue radiation dose, however, remains a matter of concern, especially in high-dose RIT [27] and repeated RIT.

Conclusion

The results of this study show that the blood, tissue and WB biodistributions and kinetics of ^{131}I -rituximab remain constant in individual patients after successive injections of radiolabelled antibody in combination with standard, weekly injections of unlabelled antibody. The results thus suggest that dosimetry studies are relevant for subsequent therapies not only with respect to WB kinetics but also for biodistribution and kinetics in tissues of concern, such as kidneys or liver and possibly bone marrow. This study might thus contribute to the understanding of the correlation between pre-treatment assessment of normal tissue radiation dose and delivered radiation dose in the subsequent RIT.

Acknowledgements. We thankfully acknowledge support from the Swiss Cancer League No KFS 991-02-2000 and excellent technical assistance from the staff of the Nuclear Medicine Department.

References

1. Wiseman GA, White CA, Stabin M, Dunn WL, Erwin W, Dahlbom M, et al. Phase I/II ^{90}Y -Zevalin (yttrium-90 ibritumomab tiuxetan, IDEC-Y2B8) radioimmunotherapy dosimetry results in relapsed or refractory non-Hodgkin's lymphoma. *Eur J Nucl Med* 2000;27:766–77.
2. Gordon LI, Molina A, Witzig T, Emmanouilides C, Raubitschek A, Darif M, et al. Durable responses after ibritumomab tiuxetan radioimmunotherapy for CD20+ B-cell lymphoma: long term follow-up of a phase I/II study. *Blood* 2004;103:4429–31.
3. Wahl RL, Zasadny KR, MacFarlane D, Francis IR, Ross CW, Estes J, et al. Iodine-131 anti-B1 antibody for B-cell lymphoma: an update on the Michigan phase I experience. *J Nucl Med* 1998;39:21S–7S.
4. Kaminski MS, Estes J, Zasadny KR, Francis IR, Ross CW, Tuck M, et al. Radioimmunotherapy with iodine (^{131}I) tositumomab for relapsed or refractory B-cell non-Hodgkin lymphoma: updated results and long-term follow-up of the University of Michigan experience. *Blood* 2000;96:1259–66.
5. Gopal AK, Gooley TA, Maloney DG, Petersdorf SH, Eary JF, Rajendran JG, et al. High-dose radioimmunotherapy versus conventional high-dose therapy and autologous hematopoietic stem cell transplantation for relapsed follicular non-Hodgkin lymphoma: a multivariable cohort analysis. *Blood* 2003;102:2351–7.
6. Juweid ME. Radioimmunotherapy of B-cell non-Hodgkin's lymphoma: from clinical trials to clinical practice. *J Nucl Med* 2002;43:1507–29.
7. Goldenberg DM. The role of radiolabeled antibodies in the treatment of non-Hodgkin's lymphoma: the coming of age of radioimmunotherapy. *Crit Rev Oncol Hematol* 2001;39:195–201.
8. Press OW, Rasey J. Principles of radioimmunotherapy for hematologists and oncologists. *Semin Oncol* 2000;27:62–73.
9. Behr TM, Griesinger F, Riggert J, Gratz S, Béhé M, Kaufmann CC, et al. High-dose myeloablative radioimmunotherapy of mantle cell non-Hodgkin lymphoma with the iodine-131-labeled chimeric anti-CD20 antibody C2B8 and autologous stem cell support. Results of a pilot study. *Cancer* 2002;94:1363–72.
10. Scheidhauer K, Wolf I, Baumgartl HJ, Von Schilling C, Schmidt B, Reidel G, et al. Biodistribution and kinetics of ^{131}I -labelled anti-CD20 MAB IDEC-C2B8 (rituximab) in relapsed non-Hodgkin's lymphoma. *Eur J Nucl Med Mol Imaging* 2002;29:1276–82.
11. Turner JH, Martindale AA, Boucek J, Claringbold PG, Leahy MF. ^{131}I -Anti CD20 radioimmunotherapy of relapsed or refractory non-Hodgkin's lymphoma: a phase II clinical trial of a non-myeloablative dose regimen of chimeric rituximab radiolabeled in a hospital. *Cancer Biother Radiopharm* 2003;18:513–24.
12. McDevitt MR, Ma D, Lai LT, Simon J, Borchardt P, Frank RK, et al. Tumor therapy with targeted atomic nanogenerators. *Science* 2001;294:1537–40.
13. Beyer GJ, Miederer M, Vranjes-Duric S, Comor JJ, Kunzi G, Hartley O, et al. Targeted alpha therapy in vivo: direct evidence for single cancer cell kill using ^{149}Tb -rituximab. *Eur J Nucl Med Mol Imaging* 2004;31:547–54.
14. Berinstein NL, Grillo-Lopez AJ, White CA, Bence-Bruckler I, Maloney D, Czuczman M, et al. Association of serum rituximab (IDEC-C2B8) concentration and anti-tumor response in the treatment of recurrent low-grade or follicular non-Hodgkin's lymphoma. *Ann Oncol* 1998;9:995–1001.
15. Maloney DG, Grillo-Lopez AJ, Bodkin DJ, White CA, Liles TM, Royston I, et al. IDEC-C2B8: results of a phase I multiple-dose trial in patients with relapsed non-Hodgkin's lymphoma. *J Clin Oncol* 1997;15:3266–74.
16. Schaffland AO, Buchegger F, Kosinski M, Antonescu C, Paschoud C, Grannavel C, et al. ^{131}I -Rituximab: relationship of immunoreactivity with specific activity. *J Nucl Med* 2004;45:1784–90.
17. Reff ME, Carner K, Chambers KS, Chinn PC, Leonard JE, Raab R, et al. Depletion of B cells in vivo by a chimeric mouse human monoclonal antibody to CD20. *Blood* 1994;83:435–45.
18. Lindmo T, Boven E, Cuttitta F, Fedorko J, Bunn PA Jr. Determination of the immunoreactive fraction of radiolabeled monoclonal antibodies by linear extrapolation to binding at infinite antigen excess. *J Immunol Methods* 1984;72:77–89.
19. Wahl RL, Kroll S, Zasadny KR. Patient-specific whole-body dosimetry: principles and a simplified method for clinical implementation. *J Nucl Med* 1998;39:14S–20S.
20. Stabin MG. MIRDOSE: personal computer software for internal dose assessment in nuclear medicine. *J Nucl Med* 1996;37:538–46.
21. Sgouros G. Bone marrow dosimetry for radioimmunotherapy: theoretical considerations. *J Nucl Med* 1993;34:689–94.
22. Scatchard G. The attractions of proteins for small molecules and ions. *Ann N Y Acad Sci* 1949;51:660–72.
23. Maloney DG, Grillo-Lopez AJ, White CA, Bodkin D, Schilder RJ, Neidhart JA, et al. IDEC-C2B8 (rituximab) anti-CD20 monoclonal antibody therapy in patients with relapsed low-grade non-Hodgkin's lymphoma. *Blood* 1997;90:2188–95.
24. Davies AJ, Rohatiner AZ, Howell S, Britton KE, Owens SE, Micallef IN, et al. Tositumomab and iodine I 131 tositumomab for recurrent indolent and transformed B-cell non-Hodgkin's lymphoma. *J Clin Oncol* 2004;22:1469–79.
25. Divgi CR, O'Donoghue JA, Welt S, O'Neil J, Finn R, Motzer RJ, et al. Phase I clinical trial with fractionated radioimmunotherapy using ^{131}I -labeled chimeric G250 in metastatic renal cancer. *J Nucl Med* 2004;45:1412–21.
26. Britton KE. Radioimmunotherapy of non-Hodgkin's lymphoma. *J Nucl Med* 2004;45:924–5.
27. Eary JF, Krohn KA, Press OW, Durack L, Bernstein ID. Importance of pre-treatment radiation absorbed dose estimation for radioimmunotherapy of non-Hodgkin's lymphoma. *Nucl Med Biol* 1997;24:635–8.